Instability in the Hartmann-Hahn double resonance

Roei Levi, Sergei Masis ⊙, and Eyal Buks ⊙

Andrew and Erna Viterbi Department of Electrical Engineering, Technion, Haifa 32000, Israel

The Hartmann-Hahn technique allows sensitivity enhancement of magnetic resonance imaging and spectroscopy by coupling the spins under study to another spin species that is externally driven. Here we theoretically study the coupled spins' dynamics and find that for a certain region of driving parameters the system becomes unstable. The required conditions for making this region of instability becoming experimentally accessible are discussed.

I. INTRODUCTION

The technique of cross-polarization (CP) [1] is widely employed in magnetic resonance imaging for sensitivity enhancement. Significant CP can be achieved by applying the so-called Hartmann-Hahn double resonance (HHDR) [2]. Near the HHDR, magnetization can be efficiently transferred between different spin species [3]. Commonly, CP is implemented to enhance the detection sensitivity of a given spin species under study by applying external driving to another ancilla spin species having higher polarization. When the Rabi frequency of the ancilla spins matches the Larmor frequency of the spins under study the so-called Hartmann-Hahn (HH) matching condition is satisfied [4] (note that this is not the same as the matching condition given by Eq. (4) of Ref. [2]). In that region a significant CP can be obtained. In thermal equilibrium the initial polarization of the ancilla spins is determined by their gyromagnetic ratio and the temperature [5,6]. The initial polarization can be further enhanced when the technique of optically induced spin polarization (OISP) can be applied [7].

Here we theoretically study back-reaction effects near the HHDR. A stability analysis is performed by a linearization of the coupled Bloch equations for the two spins, one of which is externally driven. We calculate a correction to the effective damping rate of the undriven spin, which is induced by the coupling to the driven one. Analytical results are validated against numerical calculations. A region of instability, inside which the two-spin system is expected to exhibit self-excited oscillation (SEO), is identified. The experimental feasibility of reaching this instability region is discussed. Related effects of Sisyphus cooling, amplification, lasing, and SEO have been theoretically predicted in other systems having a similar retarded response [8–13].

II. DIPOLAR BACK-REACTION

Consider two two-level systems (TLS) having a mutual coupling that is characterized by a coupling coefficient g. The first TLS, which is labeled as "a," has a relatively low angular frequency ω_{a0} in comparison with the angular fre-

quency ω_{b0} of the second TLS, which is labeled as "b" and which is externally driven. It is assumed that the state of the system can be characterized by the vector of coordinates $\bar{P} = (P_1, P_2, P_3, P_4, P_5, P_6)^{\mathrm{T}}$, where $(P_1, P_2, P_3) = (P_{a+}, P_{a-}, P_{az})$ and $(P_4, P_5, P_6) = (P_{b+}, P_{b-}, P_{bz})$ are the Bloch vectors of the first and the second TLS, respectively. It is further assumed that the vector of coordinates $\bar{P}$ satisfies a set of coupled Bloch equations [14], which are expressed as

$$\frac{dP_n}{dt} + \Theta_n(\bar{P}) = F_n, \quad (1)$$

where $n \in \{1, 2, \ldots, 6\}$, the functions $\Theta_n(\bar{P})$ (to be specified later) are time independent (which is possible provided that a rotating frame is used for the driven TLS), and F_n represent the fluctuating noise terms having vanishing average values. Let $\bar{P}_0$ be a fixed point, for which $\Theta_n(\bar{P}_0) = 0$ for all $n \in \{1, 2, \ldots, 6\}$. Fluctuations around the fixed point are governed by

$$\frac{d\bar{P}'}{dt} + J\bar{P}' = \bar{F}, \quad (2)$$

where the vector of relative coordinates $\bar{P}' = (P'_1, P'_2, P'_3, P'_4, P'_5, P'_6)^{\mathrm{T}}$ is defined by $\bar{P}' = \bar{P} - \bar{P}_0$, the vector of noise terms $\bar{F}$ is given by $\bar{F} = (F_1, F_2, F_3, F_4, F_5, F_6)^{\mathrm{T}}$, and the 6×6 Jacobian matrix J at the fixed point $\bar{P}_0$ is defined by $J_{m,n} = \partial \Theta_m / \partial P_n$. The Jacobian matrix J at the fixed point is expressed in a block form as

$$J = \left(\begin{array}{c|c} J_x & gV_{xy} \\ \hline gV_{yx} & J_y \end{array} \right). \quad (3)$$

The subspace corresponding to the subscript x (y) is henceforth referred to as the system (ancilla) subspace. For convenience, the system subspace is chosen to be of dimension 2 (corresponding to the transverse variables P_{a+} and P_{a-} of spin "a") and the ancilla subspace of dimension 4 (corresponding to the variables P_{az}, P_{b+}, P_{b-}, and P_{bz}).

Applying the Fourier transform to Eq. (2) yields (the Fourier angular frequency is denoted by ω and lowercase f and p denote the Fourier transform of uppercase F and P

variables, respectively)

$$\left(\begin{array}{c|c} J_{\mathrm{x}} - i\omega & gV_{\mathrm{xy}} \\ \hline gV_{\mathrm{yx}} & J_{\mathrm{y}} - i\omega \end{array}\right) \left(\begin{array}{c} \bar{p}_{\mathrm{x}}(\omega) \\ \bar{p}_{\mathrm{y}}(\omega) \end{array}\right) = \left(\begin{array}{c} \bar{f}_{\mathrm{x}}(\omega) \\ \bar{f}_{\mathrm{y}}(\omega) \end{array}\right), \quad (4)$$

where

$$\bar{p}_{\mathrm{x}}(\omega) = [p_1(\omega), p_1^*(-\omega)]^{\mathrm{T}},$$

$$\bar{p}_{\mathrm{y}}(\omega) = [p_3(\omega), p_4(\omega), p_4^*(-\omega), p_6(\omega)]^{\mathrm{T}},$$

and

$$\bar{f}_{\mathrm{x}}(\omega) = [f_1(\omega), f_1^*(-\omega)]^{\mathrm{T}},$$

$$\bar{f}_{\mathrm{y}}(\omega) = [f_3(\omega), f_4(\omega), f_4^*(-\omega), f_6(\omega)]^{\mathrm{T}},$$

note that the $n = 2$ ($n = 5$) equation of (1) is the complex conjugate of the $n = 1$ ($n = 4$) equation of (1). Multiplying the first [second] row of blocks of Eq. (4) by $\chi_{\mathrm{x}}(\omega) \equiv (J_{\mathrm{x}} - i\omega)^{-1}$ [$\chi_{\mathrm{y}}(\omega) \equiv (J_{\mathrm{y}} - i\omega)^{-1}$] yields $\bar{p}_{\mathrm{x}}(\omega) + g\chi_{\mathrm{x}}(\omega)V_{\mathrm{xy}}\bar{p}_{\mathrm{y}}(\omega) = \chi_{\mathrm{x}}(\omega)\bar{f}_{\mathrm{x}}(\omega)$ and $\bar{p}_{\mathrm{y}}(\omega) + g\chi_{\mathrm{y}}(\omega)V_{\mathrm{yx}}\bar{p}_{\mathrm{x}}(\omega) = \chi_{\mathrm{y}}(\omega)\bar{f}_{\mathrm{y}}(\omega)$, and thus $\bar{p}_{\mathrm{x}}(\omega)$ can be expressed as $\bar{p}_{\mathrm{x}}(\omega) = \chi_{\mathrm{x,eff}}(\omega)\bar{f}_{\mathrm{x}}(\omega)$, where $\chi_{\mathrm{x,eff}}(\omega)$ is given by

$$\begin{aligned} \chi_{\mathrm{x,eff}}(\omega) &= [1 - g^2\chi_{\mathrm{x}}(\omega)V_{\mathrm{xy}}\chi_{\mathrm{y}}(\omega)V_{\mathrm{yx}}]^{-1}\chi_{\mathrm{x}}(\omega) \\ &= [J_{\mathrm{x}} - i\omega - g^2 V_{\mathrm{xy}}\chi_{\mathrm{y}}(\omega)V_{\mathrm{yx}}]^{-1}. \end{aligned} \quad (5)$$

The term proportional to $\bar{f}_{\mathrm{y}}(\omega)$ is disregarded, since it does not affect the expectation value of $\chi_{\mathrm{x,eff}}(\omega)$.

The expression for $\chi_{\mathrm{x,eff}}(\omega)$ given by Eq. (5) suggests that the coupling effectively shifts the complex resonance frequency of the undriven spin (i.e., the first TLS labeled as "a"). To lowest nonvanishing order in the coupling coefficient g, the underlying mechanism responsible for this shift, as revealed by Eq. (5), is a three-step feedback process. In the first step, consider the case where spin "a" undergoes precession with small amplitude at its own Larmor (i.e., resonance) frequency. The term gV_{yx} in Eq. (5) represents the driving applied to the ancilla system due to the precession of spin a, and the term $\chi_{\mathrm{y}}(\omega)$ in Eq. (5) represents the corresponding response of the ancilla to this driving (the second step). This response of the ancilla gives rise to a feedback driving applied to spin a occurring in the third step, where the feedback coupling is represented by the term gV_{xy} in Eq. (5).

The coupling-induced feedback driving applied to spin a can be expressed as a sum of two orthogonal quadratures, both oscillating at the Larmor frequency of spin a. The first one is in-phase with the precession of spin a, and the second one, which occurs due to retardation in the response of the ancilla to the precession of spin a, is out of phase. The in-phase quadratures give rise to a change in the real part of the effective resonance frequency of the undriven spin a (i.e., a change in its effective Larmor frequency), whereas the change in the effective damping rate is proportional to the amplitude of the out of phase quadrature.

In general, dipolar interaction is represented by a Hamiltonian $\mathcal{H}_{\mathrm{d}}$ containing terms proportional to operators having the form $S_{\mathrm{a},i}S_{\mathrm{b},j}$, where $S_{\mathrm{a},i}$ ($S_{\mathrm{b},j}$) is the ith (jth) component of the spin a (b) angular momentum operator $\mathbf{S}_{\mathrm{a}}$ ($\mathbf{S}_{\mathrm{b}}$) (see Ref. [3], p. 66). Terms proportional to the longitudinal component of $\mathbf{S}_{\mathrm{a}}$ are disregarded since they do not contribute to effective driving at the Larmor frequency of spin a. Moreover, terms proportional to transverse components of $\mathbf{S}_{\mathrm{b}}$ can

be disregarded as well, provided that the Larmor frequency of spin b is much higher than the Larmor frequency of spin a. In this limit the driving applied to spin b due to the precession of spin a can be considered as slow, and consequently its transverse component has a weak effect compared to the effect of its longitudinal component (which effectively modulates the Larmor frequency of spin b). When only dominant terms are kept the dipolar coupling Hamiltonian $\mathcal{H}_{\mathrm{d}}$ becomes $\mathcal{H}_{\mathrm{d}} = 2g\hbar^{-1}(S_{\mathrm{a}+} + S_{\mathrm{a}-})S_{\mathrm{bz}}$.

The Hamiltonian $\mathcal{H}$ of the closed system is given by

$$\mathcal{H} = \omega_{\mathrm{a}0}S_{\mathrm{az}} + \omega_{\mathrm{b}0}S_{\mathrm{bz}} + \omega_{\mathrm{b}1}(S_{\mathrm{b}+} + S_{\mathrm{b}-}) + \mathcal{H}_{\mathrm{d}}, \quad (6)$$

where the driving amplitude and angular frequency are denoted by $\omega_{\mathrm{b}1}$ and $\omega_{\mathrm{p}} = \omega_{\mathrm{b}0} + \Delta_{\mathrm{b}}$, respectively ($\Delta_{\mathrm{b}}$ is the driving detuning), the operators $S_{\mathrm{a}\pm}$ are given by $S_{\mathrm{a}\pm} = S_{\mathrm{ax}} \pm iS_{\mathrm{ay}}$, and the rotated operators $S_{\mathrm{b}\pm}$ are given by $S_{\mathrm{b}\pm} = (S_{\mathrm{bx}} \pm iS_{\mathrm{by}})e^{\mp i\omega_{\mathrm{p}}t}$. The Heisenberg equation of motion $dO/dt = -i\hbar^{-1}[O, \mathcal{H}] + \partial O/\partial t$, where O is a given observable, together with the spin commutation relations $[S_z, S_\pm] = \pm\hbar S_\pm$ and $[S_+, S_-] = 2\hbar S_z$ yield (overdot denotes a time derivative) $\dot{S}_{\mathrm{a}+} - i\omega_{\mathrm{a}0}S_{\mathrm{a}+} + 4ig\hbar^{-1}S_{\mathrm{az}}S_{\mathrm{bz}} = 0$, $\dot{S}_{\mathrm{az}} + 2ig\hbar^{-1}(S_{\mathrm{a}+} - S_{\mathrm{a}-})S_{\mathrm{bz}} = 0$, $\dot{S}_{\mathrm{b}+} + i[\Delta_{\mathrm{b}} - 2g\hbar^{-1}(S_{\mathrm{a}+} + S_{\mathrm{a}-})]S_{\mathrm{b}+} + 2i\omega_{\mathrm{b}1}S_{\mathrm{bz}} = 0$, and $\dot{S}_{\mathrm{bz}} + i\omega_{\mathrm{b}1}(S_{\mathrm{b}+} - S_{\mathrm{b}-}) = 0$.

The interaction with the environment is accounted for by assuming that the closed system is weakly coupled to thermal baths at thermal equilibrium. The coupling turns the deterministic equations of motion for the spin operators into Langevin equations containing both damping and fluctuating terms. By applying thermal averaging, which is denoted by $\langle\rangle$, a set of coupled equations can be derived.

The coupling terms (i.e., the terms proportional to g) in the above-derived evolution equations for the operators $S_{\mathrm{a}+}$, S_{az}, and $S_{\mathrm{b}+}$ have the form gAB, where A (B) is an operator of spin a (b). The following holds $\langle AB \rangle = \langle A \rangle \langle B \rangle + \langle V_{AB} \rangle$, where $V_{AB} = (A - \langle A \rangle)(B - \langle B \rangle)$. In the mean-field approximation the term $\langle V_{AB} \rangle$ is disregarded. Note that the following holds $g\langle AB \rangle = g\langle A_0 \rangle \langle B_0 \rangle + O(g^2)$, where A_0 (B_0) represents the operator A (B) in the decoupling limit of $g \to 0$; hence, the mean-field approximation is consistent with our assumption that the coupling coefficient g is small. This approximation greatly simplifies the problem, since it allows the description of the dynamics in terms of the vector $\bar{P} = (P_{\mathrm{a}+}, P_{\mathrm{a}-}, P_{\mathrm{az}}, P_{\mathrm{b}+}, P_{\mathrm{b}-}, P_{\mathrm{bz}})^{\mathrm{T}}$, where $(\hbar/2)P_{\mathrm{az}} = \langle S_{\mathrm{az}} \rangle$, $(\hbar/2)P_{\mathrm{bz}} = \langle S_{\mathrm{bz}} \rangle$, $\hbar P_{\mathrm{a}\pm} = \langle S_{\mathrm{a}\pm} \rangle$, and $\hbar P_{\mathrm{b}\pm} = \langle S_{\mathrm{b}\pm} \rangle$. The vector $\bar{P}$ is determined by two real numbers P_{az} and P_{bz}, and two complex numbers $P_{\mathrm{a}+} = P_{\mathrm{a}-}^*$ and $P_{\mathrm{b}+} = P_{\mathrm{b}-}^*$, whereas more variables are needed for treating the general case (the density operator of a two-spin system is determined by 15 real numbers).

Note that for product states, for which $\langle V_{AB} \rangle = 0$, the mean-field approximation becomes exact. It can be used provided that the lifetime of entangled states is much shorter than all single spin lifetimes. When this assumption cannot be made a more general analysis, which does not exclude entanglement, is needed. The so-called concurrence [15] allows quantifying the entanglement. An expression for a critical temperature, T_{c}, above which in the steady state the spin-spin system becomes separable (i.e., entanglement vanishes)

has been derived in Refs. [16,17]. Near the HH matching condition the critical temperature is approximately given by $T_c \simeq \hbar g/k_B$, where k_B is the Boltzmann constant. Hence, for the vast majority of magnetic resonance experimental setups, for which the temperature $T \gg T_c$ (recall that g represents dipolar coupling), entanglement can be safely disregarded.

In the mean-field approximation the functions $\overline{\Theta}(\bar{P}) = (\Theta_1, \Theta_2, \Theta_3, \Theta_4, \Theta_5, \Theta_6)^T$ are given by $\Theta_1 = \Theta_2^* = (\gamma_{a2} - i\omega_{a0})P_{a+} + igP_{az}P_{bz}$, $\Theta_3 = \gamma_{a1}(P_{az} - P_{az,s}) + 2ig(P_{a+} - P_{a-})P_{bz}$, $\Theta_4 = \Theta_5^* = (\gamma_{b2} + i\Delta_b)P_{b+} + i\omega_{b1}P_{bz} - 2ig(P_{a+} + P_{a-})P_{b+}$, and $\Theta_6 = \gamma_{b1}(P_{bz} - P_{bz,s}) + 2i\omega_{b1}(P_{b+} - P_{b-})$, where γ_{a1} (γ_{b1}) is the longitudinal relaxation rate of the undriven (driven) spin, γ_{a2} (γ_{b2}) is the transverse relaxation rate of the undriven (driven) spin, $P_{az,s} = -\tanh(\hbar\omega_{a0}/2k_BT)$ $[P_{bz,s} = -\tanh(\hbar\omega_{b0}/2k_BT)]$ is the value of P_{az} (P_{bz}) in thermal equilibrium, and k_BT is the thermal energy. Note that in the steady state the expectation values of the transverse components of the undriven spin a vanish (for the decoupled case $g = 0$), i.e., $P_{a+,} = P_{a-} = 0$.

The derivation below is mainly devoted to the analytical inversion of the matrix $J_y - i\omega$, which, in turn, allows the evaluation of $\chi_{x,eff}(\omega)$ according to Eq. (5). The matrices J_x (2×2) and J_y (4×4) are given by

$$J_x = \begin{pmatrix} \gamma_{a2} - i\omega_{a0} & 0 \\ 0 & \gamma_{a2} + i\omega_{a0} \end{pmatrix}, \qquad (7)$$

$$J_y = \begin{pmatrix} \gamma_{a1} & 0 & 0 & 0 \\ 0 & \gamma_{b2} + i\Delta_b & 0 & i\omega_{b1} \\ 0 & 0 & \gamma_{b2} - i\Delta_b & -i\omega_{b1} \\ 0 & 2i\omega_{b1} & -2i\omega_{b1} & \gamma_{b1} \end{pmatrix}, \qquad (8)$$

and the coupling matrices V_{xy} (2×4) and V_{yx} (4×2) are given by

$$V_{xy} = \begin{pmatrix} iP_{bz} & 0 & 0 & iP_{az} \\ -iP_{bz} & 0 & 0 & -iP_{az} \end{pmatrix}, \qquad (9)$$

$$V_{yx} = \begin{pmatrix} 2iP_{bz} & -2iP_{bz} \\ -2iP_{b+} & -2iP_{b+} \\ 2iP_{b-} & 2iP_{b-} \\ 0 & 0 \end{pmatrix}. \qquad (10)$$

To the lowest nonvanishing order in g the blocks V_{xy} and V_{yx} are evaluated by replacing all variables $\bar{P}$ by their averaged steady-state values in the absence of coupling, which are denoted as $\bar{P}_0 = (P_{a+0}, P_{a-0}, P_{az0}, P_{b+0}, P_{b-0}, P_{bz0})$. These averaged steady-state values are evaluated in Appendix A, and it is found that [see Eq. (A9)]

$$P_{bz0} = \frac{\left(1 + \frac{\Delta_b^2}{\gamma_{b2}^2}\right)P_{bz,s}}{1 + \frac{4\omega_{b1}^2}{\gamma_{b1}\gamma_{b2}} + \frac{\Delta_b^2}{\gamma_{b2}^2}}, \qquad (11)$$

$$P_{b+0} = \frac{\frac{\omega_{b1}}{\gamma_{b2}}\left(-\frac{\Delta_b}{\gamma_{b2}} - i\right)P_{bz,s}}{1 + \frac{4\omega_{b1}^2}{\gamma_{b1}\gamma_{b2}} + \frac{\Delta_b^2}{\gamma_{b2}^2}}, \qquad (12)$$

$P_{b+0}^* = P_{b-0}$, $P_{az0} = P_{az,s}$, and $P_{a+0} = P_{a-0} = 0$ (since the first spin is not driven).

Next, the effective susceptibility matrix $\chi_{x,eff}(\omega)$ is evaluated at the resonance frequency of the first TLS ω_{a0}. The following holds [see Eq. (8)]:

$$\chi_y(\omega_{a0}) = (J_y - i\omega_{a0})^{-1} = \frac{1}{D_L}\begin{pmatrix} \frac{D_L}{D_0} & 0 & 0 & 0 \\ 0 & D_2D_3 + 2\omega_{b1}^2 & 2\omega_{b1}^2 & -i\omega_{b1}D_2 \\ 0 & 2\omega_{b1}^2 & D_1D_3 + 2\omega_{b1}^2 & i\omega_{b1}D_1 \\ 0 & -2i\omega_{b1}D_2 & 2i\omega_{b1}D_1 & D_1D_2 \end{pmatrix}, \qquad (13)$$

where $D_0 = \gamma_{a1} - i\omega_{a0}$, $D_1 = \gamma_{b2} + i\Delta_b - i\omega_{a0}$, $D_2 = \gamma_{b2} - i\Delta_b - i\omega_{a0}$, $D_3 = \gamma_{b1} - i\omega_{a0}$, and $D_L = D_1D_2D_3 + 2\omega_{b1}^2(D_1 + D_2)$. As can be seen from Eq. (5), only the diagonal elements of $V_{xy}\chi_y(\omega)V_{yx}$ contribute to the eigenvalues of $\chi_{x,eff}(\omega)$ to the lowest nonvanishing order in g (second order). To the same order the effective complex frequency of the first TLS is $\omega_{a0} + i\gamma_{a2} - i\Upsilon_a$, where

$$\Upsilon_a = g^2[V_{xy}\chi_y(\omega)V_{yx}]_{11}. \qquad (14)$$

Substituting the corresponding coupling matrices V_{xy} and V_{yx} leads to [see Eqs. (9), (10), (13), and (12)]

$$\Upsilon_a = -2g^2\left(\frac{P_{bz0}^2}{D_0} + 2i\omega_{b1}P_{az0}\frac{D_2P_{b+0} + D_1P_{b-0}}{D_L}\right). \qquad (15)$$

The determinant D_L can be expressed as $D_L/\omega_{a0}^3 = (\gamma_{b1}/\omega_{a0})\eta$, where $\eta = \eta' + i\eta''$, $\eta' = \Delta_b^2/\omega_{a0}^2 - [1 + (2\gamma_{b2}/\gamma_{b1})(1 - 2\omega_{b1}^2/\omega_{a0}^2) - \gamma_{b2}^2/\omega_{a0}^2]$, $\eta'' = [1 - (2\gamma_{b1}/\omega_{a0} + \gamma_{b2}/\omega_{a0})(\gamma_{b2}/\omega_{a0}) - \omega_R^2/\omega_{a0}^2]/(\gamma_{b1}/\omega_{a0})$, and ω_R, which is given by

$$\omega_R = \sqrt{4\omega_{b1}^2 + \Delta_b^2}, \qquad (16)$$

is the Rabi frequency of the driven spins, thus Eq. (15) can be rewritten as

$$\frac{\omega_{a0}\Upsilon_a}{2g^2} = \frac{\frac{4\left(1 + \frac{2i\gamma_{b2}}{\omega_{a0}}\right)\Delta_b\omega_{b1}^2 P_{az,s}P_{bz,s}}{\gamma_{b2}^2\gamma_{b1}\eta}}{1 + \frac{4\omega_{b1}^2}{\gamma_{b1}\gamma_{b2}} + \frac{\Delta_b^2}{\gamma_{b2}^2}} + \frac{\left(1 + \frac{\Delta_b^2}{\gamma_{b2}^2}\right)\left(\frac{\gamma_{a1}}{\omega_{a0}} - i\right)P_{bz,s}^2}{\left(1 + \frac{4\omega_{b1}^2}{\gamma_{b1}\gamma_{b2}} + \frac{\Delta_b^2}{\gamma_{b2}^2}\right)^2\left(1 + \frac{\gamma_{a1}^2}{\omega_{a0}^2}\right)}. \qquad (17)$$

The effective damping rate of spin a is given by $\gamma_{a2}(1 + \alpha_a)$, where $\alpha_a = -\mathrm{Re}(\Upsilon_a)/\gamma_{a2}$. The contribution of the term in the second line of Eq. (17) to α_a can be disregarded provided that $\gamma_{a1} \ll \omega_{a0}$.

The dependence according to Eq. (17) of α_a on the normalized detuning Δ_b/ω_{a0} and on the normalized driving amplitude ω_{b1}/ω_{a0} is shown in Fig. 1(a) (the term proportional to P_{bz0}^2 is disregarded since it is assumed that $\gamma_{a1} \ll \omega_{a0}$). The parameters that have been used for generating the plot are listed
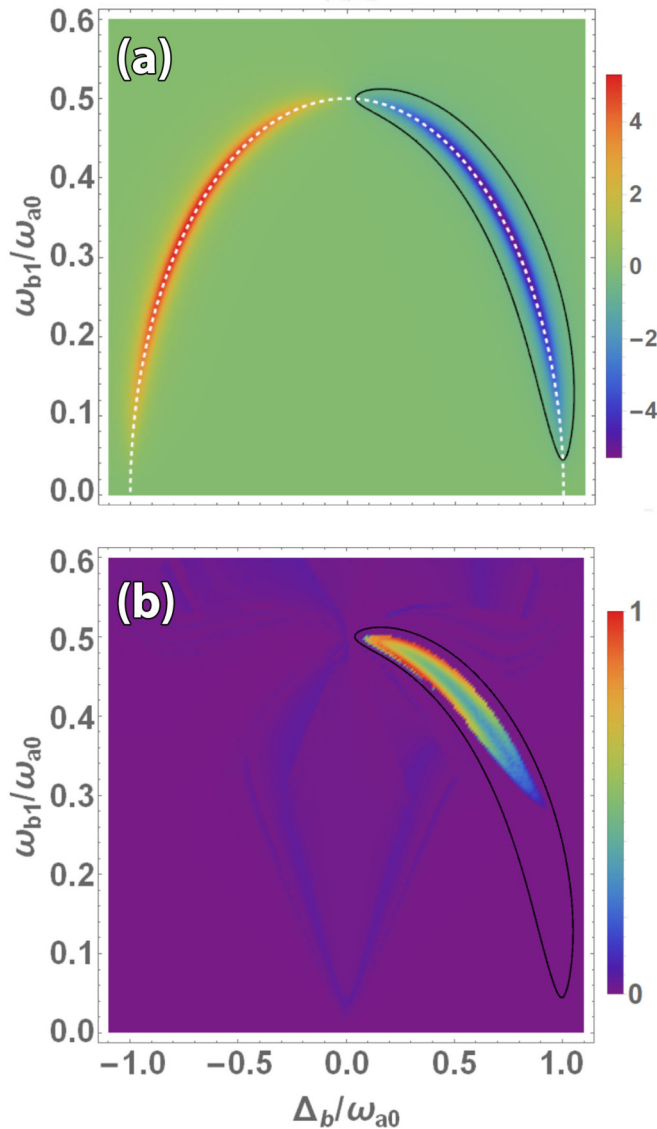
FIG. 1. The effective damping rate of spin a. (a) Color-coded plot of α_a vs Δ_b/ω_{a0} and ω_{b1}/ω_{a0} with parameters $g/\omega_{a0} = 1.0$, $\gamma_{a1}/\omega_{a0} = 10^{-2}$, $\gamma_{a2}/\omega_{a0} = 10^{-4}$, $\gamma_{b1}/\omega_{a0} = 3.7 \times 10^{-3}$, $\gamma_{b2}/\omega_{a0} = 3.7 \times 10^{-2}$, $P_{az,s} = -5 \times 10^{-4}$, and $P_{bz,s} = -1$. (b) Numerical solution for the normalized steady-state amplitude of P_{a+} vs Δ_b/ω_{a0} and ω_{b1}/ω_{a0}, with the same parameters as in panel (a). The fluctuating noise terms $\bar{F}$ are disregarded in the numerical calculation.

in the figure caption. Spin b is assumed to be fully polarized, for instance, by OISP. Also, the curve along which $\alpha_a = -1$ is shown as a solid black curve on the same plot. This curve labels the border between the regions of positive and negative effective damping rates for the undriven spin. When the driving is red-detuned, i.e., when Δ_b is negative, the change in the damping rate γ_{a2} is positive, and consequently spin cooling is expected to occur [18]. The opposite behavior occurs with blue detuning, i.e., when Δ_b is positive. Specifically, SEO is expected in the area enclosed by the black curve. Along this curve the system undergoes a Hopf bifurcation [19].

For both red and blue detuning, a large change in the effective spin damping rate occurs near the overlaid dashed white line in Fig. 1, along which the Rabi frequency ω_R coincides with ω_{a0}, i.e., $\Delta_b = \pm\sqrt{\omega_{a0}^2 - 4\omega_{b1}^2}$, and the HH matching condition is satisfied. This behavior can be explained by noticing that $|\eta''| \ll 1$ along the dashed line, i.e., when $\omega_R = \omega_{a0}$, and consequently $|\alpha_a|$ obtains a peak.

The underlying mechanism responsible for the change in the effective damping rate of the undriven spin is similar to a related mechanism occurring in optomechanical cavities [18]. The change in the effective damping rate of the system under study (i.e., spin a) is attributed to the retardation in the response of the driven ancilla (i.e., spin b) to fluctuation in the state of spin a. Both effects of cooling and heating are attributed to imbalance between fluctuation and dissipation [18] occurring due to the change in the effective damping rate of spin a.

The analytic result given by Eq. (17) was validated against a numerical simulation of a time-dependent solution of the equations of motion [see Eq. (1)]. A plot for the normalized steady-state amplitude of P_{a+} vs the normalized detuning Δ_b/ω_{a0} and the normalized driving amplitude ω_{b1}/ω_{a0} is shown in Fig. 1(b). The undriven spin experiences SEO in the region of negative effective damping rate (encircled by the black curve). Deviation between the region of SEO that is obtained by the solid black curve and the one that is obtained from the numerical calculation is attributed to the term P_{bz0}^2/D_0 that was neglected in Eq. (17).

As was mentioned above, our analysis is based on the mean-field approximation, which, in turn, is based on the assumption that entanglement is nearly fully suppressed. The more general case can be explored using the system's master equation. In general, the master equation contains terms originating from the unitary evolution generated by the Hamiltonian $\mathcal{H}$ (6) of the closed system and terms originating from the interaction with the environment. In some cases only linear terms associated with the interaction with the environment are kept. For these cases the master equation can be expressed in the form given by Eq. (B5) of Appendix B. The matrix G in Eq. (B5) represents linear damping. In Appendix B we show that for these cases instabilities are excluded provided that all diagonal matrix elements of G are positive [see inequality (B9)]. This observation suggests that a master equation having the form given by Eq. (B5) is inapplicable for our case.

Grabert has shown that the invalidity of the quantum regression hypothesis gives rise to a nonlinear term in the master equation of a general quantum system [20]. This nonlinear term, which is ignored in many publications, is not included in Eq. (B5). Using general expressions derived in Refs. [21,22], we can derive a Grabert master equation for the two-spin problem under study here. Moreover, for this problem, additional nonlinear terms have to be added to the master equation [23,24], since external driving is applied, and consequently the transverse coordinates of spin b cannot be assumed to be small. In the derivation of the master equation it is important to note that additivity of decay rates may break down for bipartite decoherence [25]. Since the resultant nonlinear master equation cannot be expressed in the form given by Eq. (B5), instabilities cannot be generally excluded. Detailed analysis based on the nonlinear master equation is kept outside the scope of the current paper.

III. EXPERIMENTAL FEASIBILITY

The experimental feasibility to reach the instability threshold occurring when $\alpha_a = -1$ is discussed below. Consider the case where the HH condition $\omega_R = \omega_{a0}$ is satisfied [see the dashed white curve in Fig. 1(a)]. As is demonstrated by Fig. 1, the largest change in α_a typically occurs when the detuning $|\Delta_b|$ and and driving amplitude ω_{b1} are of the same order of magnitude (i.e., $|\Delta_b| \simeq \omega_{b1} \simeq \omega_{a0}$). When the following holds, $\omega_{a0} \ll \omega_{b0}$, $\gamma_{b1} \ll \gamma_{b2} \ll |\Delta_b|$, and $|\Delta_b| \simeq \omega_{b1} \simeq \omega_{a0}$, the threshold condition $\alpha_a = -1$ yields the requirement $\kappa P_{az,s} P_{bz,s} \simeq 1$, where $\kappa = g^2 \gamma_{b1}/(\gamma_{a2}\gamma_{b2}^2)$ is the cooperativity parameter [see Eq. (17)].

As an example, consider two nearby defects in a diamond lattice [26]. The first one having the Larmor angular frequency ω_{a0} is a negatively charged nitrogen-vacancy (NV$^-$) defect [27], and the second one is a nitrogen-substitutional defect (P1) [28] having the Larmor angular frequency ω_{b0}. An externally applied magnetic field B parallel to the NV axis can be used to tune both ω_{a0} and ω_{b0}. Two spin states belonging to the NV$^-$ spin triplet ground state become nearly degenerate near the magnetic field value of $B = 102$ mT . In that region the angular frequency ω_{b0} of the electronic-like P1 transitions is about $\omega_{b0} = \gamma_e B = 2\pi \times 2.9$ GHz, where $\gamma_e = 2\pi \times 28.03$ GHz T^{-1} is the electron spin gyromagnetic ratio. For this value of ω_{b0} the P1 electronic spin defects can be nearly fully polarized, i.e., $|P_{bz,s}| \simeq 1$, by cooling down the sample well below a temperature of about 0.07 K.

In practice, the value of the NV transition frequency ω_{a0} (which can be tuned by the externally applied magnetic field) is limited due to the HH matching condition by the maximum possible value of the driving amplitude ω_{b1} that can be experimentally achieved. For the case where a high-quality factor microwave resonator is employed for driving the P1 spins [13], a value of about $\omega_{a0} = \omega_R \simeq 2\pi \times 50$ MHz is reachable. This value is too small to allow making $|P_{az,s}|$ becoming of order unity using cooling only. However the condition $|P_{az,s}| \simeq 1$ can be satisfied using the technique of OISP [29,30].

The dipolar coupling coefficient g between the NV$^-$ electron spin and the P1 electron spin is given by $g/2\pi \simeq 3.6$ GHz $(r_d/a_d)^{-3}$ [3], where r_d is the NV$^-$-P1 distance, $a_d = 3.57$Å is the lattice constant of diamond, and it is assumed for simplicity that the angle between the line joining the two defects and the NV axis vanishes. When both spins are fully polarized and for the typical values of $\gamma_{a2} = \gamma_{b2} = 2\pi \times 0.1$ MHz and $\gamma_{b1} = 2\pi \times 0.01$ MHz, the threshold condition $\alpha_a = -1$ is satisfied when $r_d \simeq 8$ nm.

In the above example the case of dipolar coupling between two electron spins localized near different lattice sites was considered. This coupling, however, depends on the distance between sites, and consequently, its study is difficult using measurements of ensembles containing many spins. Such inhomogeneity is avoided for the case where the same lattice site hosts both spins. For that case, spin a is assumed to be a nuclear spin and spin b is an electron spin. For example, for the case of P1 defects in diamond, the dipolar coupling between the nitrogen-14 nuclear spin $S = 1$ and the spin of the localized unpaired electron occupying the same lattice site

gives rise to hyperfine splitting on the order of 100 MHz [13]. Such a coupling is sufficiently strong to make the region of SEO experimentally accessible, and the study of this instability can be performed using measurements of ensembles containing many P1 defects.

IV. SUMMARY

Our results demonstrate that a significant change in the effective value of the transverse spin relaxation rate can be induced, provided that the HH matching condition can be satisfied. Red-detuned driving provides a positive contribution to the relaxation rate, whereas a negative contribution can be obtained by blue-detuned driving. For the former case this effect can be utilized for cooling down spins, while the later case of blue detuning may allow inducing SEO. Operating close to the threshold of SEO, i.e., close to the point where the total effective damping vanishes, may be useful for sensing applications, since the system is expected to become highly responsive to external perturbations near the threshold. It is important to emphasize that our analysis is based on the mean-field approximation, and therefore our results are inapplicable for the case where entanglement cannot be disregarded.

APPENDIX A: FIXED POINTS OF BLOCH EQUATIONS

The dynamics of the polarization vector $\mathbf{P} = P_x\hat{\mathbf{x}} + P_y\hat{\mathbf{y}} + P_z\hat{\mathbf{z}}$, which describes the state of the spin system, is governed by the Bloch equation [3]

$$\frac{d\mathbf{P}}{dt} = \mathbf{P} \times \mathbf{\Omega} + \gamma, \tag{A1}$$

where $\mathbf{\Omega}(t)$ is the rotation vector, which is proportional to the externally applied magnetic field vector (the factor of proportionality is called the gyromagnetic ratio). The vector

$$\gamma = -\gamma_2 P_x \hat{\mathbf{x}} - \gamma_2 P_y \hat{\mathbf{y}} - \gamma_1 (P_z - P_{z,s})\hat{\mathbf{z}} \tag{A2}$$

represents the contribution of damping, where $\gamma_1 = 1/T_1$ and $\gamma_2 = 1/T_2$ are the longitudinal and transverse relaxation rates, respectively, and where $P_{z,s}$ is the equilibrium steady-state polarization.

Consider the case where the rotation vector $\mathbf{\Omega}(t)$ is taken to be given by

$$\mathbf{\Omega}(t) = 2\omega_1(\cos(\omega t)\hat{\mathbf{x}} + \sin(\omega t)\hat{\mathbf{y}}) + \omega_0\hat{\mathbf{z}}, \tag{A3}$$

where ω_1, ω, and ω_0 are real constants. For this case, Eq. (A1) becomes

$$\frac{d\mathbf{P}}{dt} + M_B\mathbf{P} = \begin{pmatrix} 0 \\ 0 \\ \gamma_1 P_{z,s} \end{pmatrix}, \tag{A4}$$

where

$$
M_{\mathrm{B}} = \begin{pmatrix} \gamma_2 & -\omega_0 & 2\omega_1 \sin(\omega t) \\ \omega_0 & \gamma_2 & -2\omega_1 \cos(\omega t) \\ 2\omega_1 \sin(\omega t) & -2\omega_1 \cos(\omega t) & \gamma_1 \end{pmatrix}.
$$
(A5)

The variable transformation

$$
\begin{pmatrix} P_x \\ P_y \end{pmatrix} = \begin{pmatrix} e^{i\omega t} & e^{-i\omega t} \\ -ie^{i\omega t} & ie^{-i\omega t} \end{pmatrix} \begin{pmatrix} P_+ \\ P_- \end{pmatrix}
$$
(A6)

leads to

$$
\frac{d}{dt} \begin{pmatrix} P_+ \\ P_- \\ P_z \end{pmatrix} + J \begin{pmatrix} P_+ \\ P_- \\ P_z \end{pmatrix} = \begin{pmatrix} 0 \\ 0 \\ \gamma_1 P_{z,\mathrm{s}} \end{pmatrix},
$$
(A7)

where

$$
J = \begin{pmatrix} \gamma_2 - i\Delta & 0 & i\omega_1 \\ 0 & \gamma_2 + i\Delta & -i\omega_1 \\ 2i\omega_1 & -2i\omega_1 & \gamma_1 \end{pmatrix},
$$
(A8)

and where $\Delta = \omega - \omega_0$ is the driving detuning. The steady-state solution of Eq. (A7) is given by

$$
\begin{pmatrix} P_{+0} \\ P_{-0} \\ P_{z0} \end{pmatrix} = J^{-1} \begin{pmatrix} 0 \\ 0 \\ \gamma_1 P_{z,\mathrm{s}} \end{pmatrix}
$$

$$
= \begin{pmatrix} \dfrac{\frac{\omega_1}{\gamma_2}\left(-\frac{\Delta}{\gamma_2}-i\right)}{1+\frac{4\omega_1^2}{\gamma_1\gamma_2}+\frac{\Delta^2}{\gamma_2^2}} \\[3ex] \dfrac{\frac{\omega_1}{\gamma_2}\left(-\frac{\Delta}{\gamma_2}+i\right)}{1+\frac{4\omega_1^2}{\gamma_1\gamma_2}+\frac{\Delta^2}{\gamma_2^2}} \\[3ex] \dfrac{1+\frac{\Delta^2}{\gamma_2^2}}{1+\frac{4\omega_1^2}{\gamma_1\gamma_2}+\frac{\Delta^2}{\gamma_2^2}} \end{pmatrix} P_{z,\mathrm{s}}.
$$
(A9)

APPENDIX B: LINEAR MASTER EQUATION

Consider a closed quantum system having a Hilbert space of dimension d_{H}, whose Hamiltonian is given by $\mathcal{H} \doteq \hbar \Omega_{\mathrm{H}}$, where the $d_{\mathrm{H}} \times d_{\mathrm{H}}$ matrix Ω_{H} is Hermitian and time independent. It is assumed that the master equation for the system's reduced density matrix ρ can be expressed as

$$
\frac{d\rho}{dt} = i[\rho, \Omega_{\mathrm{H}}] - \gamma_{\mathrm{E}}[Q, [Q, \rho]]
$$
$$
- \eta_{\mathrm{E}} \gamma_{\mathrm{E}} [Q, [Q, \Omega_{\mathrm{H}}]],
$$
(B1)

where the coefficient $\gamma_{\mathrm{E}} > 0$ is a damping rate, $\eta_{\mathrm{E}} > 0$ is dimensionless, and the dimensionless Hermitian matrix Q represents the interaction with the system's environment. In this Appendix it is shown that any master equation having this form is stable provided that d_{H} is finite.

The density matrix can be expressed as

$$
\rho = \frac{1}{d_{\mathrm{H}}} + \bar{k} \cdot \bar{\lambda},
$$
(B2)

where $\bar{k} = (k_1, k_2, \ldots, k_{d_{\mathrm{H}}^2-1})$ and $\bar{\lambda} = (\lambda_1, \lambda_2, \ldots, \lambda_{d_{\mathrm{H}}^2-1})$. The $d_{\mathrm{H}}^2 - 1$ Hermitian and trace-less $d_{\mathrm{H}} \times d_{\mathrm{H}}$ matrices λ_n, which span the SU(d_{H}) Lie algebra, satisfy the orthogonality relation

$$
\frac{\mathrm{Tr}(\lambda_a \lambda_b)}{2} = \delta_{ab}.
$$
(B3)

For example, for the case of the two-level (three-level) system, i.e. for $d_{\mathrm{H}} = 2$ ($d_{\mathrm{H}} = 3$), the $d_{\mathrm{H}}^2 - 1 = 3$ Pauli ($d_{\mathrm{H}}^2 - 1 = 8$ Gell-Mann) matrices can be used. Note that the condition $\mathrm{Tr}\,\rho^2 = d_{\mathrm{H}}^{-1} + 2|\bar{k}|^2 \leqslant 1$ implies that $|\bar{k}|^2 \leqslant (1 - d_{\mathrm{H}}^{-1})/2$.

With the help of the orthogonality relation (B3) and the general trace identity $\mathrm{Tr}(XY) = \mathrm{Tr}(YS)$ the master equation (B1) can be expressed as (repeated index implies summation)

$$
\frac{dk_a}{dt} = \frac{i}{2} \mathrm{Tr}(\Omega_{\mathrm{H}}([\lambda_a, \lambda_b]))k_b
$$
$$
- \frac{\gamma_{\mathrm{E}}}{2} \mathrm{Tr}(-[Q, \lambda_b][Q, \lambda_a])k_b
$$
$$
- \frac{\eta_{\mathrm{E}} \gamma_{\mathrm{E}}}{2} \mathrm{Tr}([Q, [Q, \Omega_{\mathrm{H}}]]\lambda_a)
$$
(B4)

or in a matrix form as

$$
\frac{d\bar{k}}{dt} = (M - G)\bar{k} + \bar{k}_0.
$$
(B5)

The $(d_{\mathrm{H}}^2 - 1) \times (d_{\mathrm{H}}^2 - 1)$ matrix M, which represents the unitary evolution governed by the Hamiltonian of the closed system $\mathcal{H}$, is given by $M_{a,b} = (i/2)\mathrm{Tr}(\Omega_{\mathrm{H}}[\lambda_a, \lambda_b])$ [see Eq. (B4)]. Note that the matrix M is *real* and *antisymmetric* (or skew symmetric), i.e., $M^{\mathrm{T}} = -M$. This implies that $\det(M^{\mathrm{T}}) = \det(-M) = (-1)^{d_{\mathrm{H}}^2-1} \det M$, and hence $\det M = 0$ for odd $d_{\mathrm{H}}^2 - 1$. Note also that when interaction with the environment is disregarded, i.e., when $\gamma_{\mathrm{E}} = 0$, the following holds: $(d\bar{k}/dt) \cdot \bar{k} = 0$; i.e., for this dissipationless case the magnitude $|\bar{k}|$ of the vector $\bar{k}$ is a constant of the motion.

The $(d_{\mathrm{H}}^2 - 1) \times (d_{\mathrm{H}}^2 - 1)$ matrix G, which represents linear damping, is given by $G_{a,b} = (\gamma_{\mathrm{E}}/2)\mathrm{Tr}(-[Q, \lambda_b][Q, \lambda_a])$ [see Eq. (B4)]. The elements of the vector $\bar{k}_0$ are given by $(\bar{k}_0)_a = (-\eta_{\mathrm{E}} \gamma_{\mathrm{E}}/2)\mathrm{Tr}([Q, [Q, \Omega_{\mathrm{H}}]]\lambda_a)$. Note that all elements of G and $\bar{k}_0$ are *real* (recall that, in general, $i[A, B]$ is Hermitian provided that both A and B are Hermitian). Moreover, all *diagonal* elements of G are *positive* (note that $-[Q, \lambda_b][Q, \lambda_a]$ is positive definite for the case $a = b$).

The solution of Eq. (B5) is given by

$$
\bar{k}(t) = e^{(M-G)t}\bar{k}(0) + \int_0^t dt'\, e^{(M-G)(t-t')}\bar{k}_0.
$$
(B6)

The system's stability depends on the set of eigenvalues of the matrix $M - G$, which is denoted by $\mathcal{S}$. The system is stable provided that $\mathrm{real}(\xi) < 0$ for any $\xi \in \mathcal{S}$. For that case the steady-state solution is given by $-(M - G)^{-1}\bar{k}_0$.

Let $v = v' + iv''$ be an eigenvector of $M - G$ with eigenvalue $\xi = \xi' + i\xi''$, where $\xi', \xi'' \in \mathbb{R}$ and $v', v'' \in \mathbb{R}^{d_{\mathrm{H}}^2-1}$ ($\mathbb{R}$ denotes the set of real numbers):

$$
(M - G)v = \xi v.
$$
(B7)

It is shown below that the system is stable, i.e., $\mathrm{real}(\xi) = \xi' < 0$ for any $\xi \in \mathcal{S}$, provided that both M and G are real, M is antisymmetric, and all diagonal elements of G are positive.

The matrix G can be decomposed as $G = \mathcal{A} + \mathcal{T} + \mathcal{D}$, where $\mathcal{A}$ is antisymmetric, $\mathcal{T}$ is upper triangular, and $\mathcal{D}$ is diagonal. The following holds: $\mathcal{A}_{n,m} = G_{n,m}$ and $\mathcal{T}_{n,m} = 0$ for $n > m$; $\mathcal{A}_{n,m} = -G_{m,n}$ and $\mathcal{T}_{n,m} = G_{n,m} + G_{m,n}$ for $n < m$; and for the diagonal elements $\mathcal{A}_{n,n} = \mathcal{T}_{n,n} = 0$ and $\mathcal{D}_{n,n} = G_{n,n}$. Using this notation one has $M - G = \mathcal{M} - \mathcal{P}$, where $\mathcal{M} = M - \mathcal{A}$ and $\mathcal{P} = \mathcal{T} + \mathcal{D}$. As was shown above, M is antisymmetric provided that the Hamiltonian $\mathcal{H}$ is Hermitian, hence $\mathcal{M}$ is antisymmetric as well. The eigenvalues of the upper triangular matrix $\mathcal{P}$ are the diagonal elements of G, hence $\mathcal{P}$ is positive definite provided that all diagonal elements of the matrix G are positive.

The real and imaginary parts of Eq. (B7) are given by $(\mathcal{M} - \mathcal{P})v' = \xi'v' - \xi''v''$ and $(\mathcal{M} - \mathcal{P})v'' = \xi'v'' + \xi''v'$, respectively; hence, the following holds: $(v')^{\mathrm{T}}(\mathcal{M} - \mathcal{P})v' + (v'')^{\mathrm{T}}(\mathcal{M} - \mathcal{P})v'' = \xi'((v')^{\mathrm{T}}v' + (v'')^{\mathrm{T}}v'')$ or (recall that $\mathcal{M}$ is antisymmetric)

$$
\begin{aligned}
\xi' &= \frac{(v')^{\mathrm{T}}(\mathcal{M} - \mathcal{P})v' + (v'')^{\mathrm{T}}(\mathcal{M} - \mathcal{P})v''}{(v')^{\mathrm{T}}v' + (v'')^{\mathrm{T}}v''} \\
&= -\frac{(v')^{\mathrm{T}}\mathcal{P}v' + (v'')^{\mathrm{T}}\mathcal{P}v''}{(v')^{\mathrm{T}}v' + (v'')^{\mathrm{T}}v''},
\end{aligned} \tag{B8}
$$

thus

$$
\xi' \leqslant -\min G_{n,n} < 0, \tag{B9}
$$

hence the system is stable.

[1] A. Pines, M. G. Gibby, and J. S. Waugh, Proton-enhanced NMR of dilute spins in solids, J. Chem. Phys. **59**, 569 (1973).

[2] S. R. Hartmann and E. L. Hahn, Nuclear double resonance in the rotating frame, Phys. Rev. **128**, 2042 (1962).

[3] C. P. Slichter, *Principles of Magnetic Resonance*, Springer Series in Solid-State Sciences Vol. 1 (Springer, Berlin, 2013).

[4] P. Yang, M. B. Plenio, and J. Cai, Dynamical nuclear polarization using multi-colour control of color centers in diamond, EPJ Quantum Technol. **3**, 1 (2016).

[5] A. Abragam and W. G. Proctor, Spin temperature, Phys. Rev. **109**, 1441 (1958).

[6] A. Abragam, *The Principles of Nuclear Magnetism*, Internationals Series of Monographs on Physics Number 32 (Oxford University Press, Oxford, 1961).

[7] P. London, J. Scheuer, J.-M. Cai, I. Schwarz, A. Retzker, M. B. Plenio, M. Katagiri, T. Teraji, S. Koizumi, J. Isoya, R. Fischer, L. P. McGuinness, B. Naydenov, and F. Jelezko, Detecting and Polarizing Nuclear Spins with Double Resonance on a Single Electron Spin, Phys. Rev. Lett. **111**, 067601 (2013).

[8] R. Glenn and M. E. Raikh, Rabi-vibronic resonance with large number of vibrational quanta, Phys. Rev. B **84**, 195454 (2011).

[9] M. Grajcar, S. H. W. Van der Ploeg, A. Izmalkov, E. Il'ichev, H.-G. Meyer, A. Fedorov, A. Shnirman, and G. Schön, Sisyphus cooling and amplification by a superconducting qubit, Nat. Phys. **4**, 612 (2008).

[10] J. M. De Voogd, J. J. T. Wagenaar, and T. H. Oosterkamp, Dissipation and resonance frequency shift of a resonator magnetically coupled to a semiclassical spin, Sci. Rep. **7**, 42239 (2017).

[11] L. Ella and E. Buks, Hopf bifurcation in a flux qubit coupled to a nanomechanical oscillator, arXiv:1210.6902.

[12] T. Ramos, V. Sudhir, K. Stannigel, P. Zoller, and T. J. Kippenberg, Nonlinear Quantum Optomechanics via Individual Intrinsic Two-Level Defects, Phys. Rev. Lett. **110**, 193602 (2013).

[13] H. Wang, S. Masis, R. Levi, O. Shtempluk, and E. Buks, Off-resonance coupling between a cavity mode and an ensemble of driven spins, Phys. Rev. A **95**, 053853 (2017).

[14] I. Solomon, Relaxation processes in a system of two spins, Phys. Rev. **99**, 559 (1955).

[15] W. K. Wootters, Entanglement of Formation of an Arbitrary State of Two Qubits, Phys. Rev. Lett. **80**, 2245 (1998).

[16] L. Quiroga, F. J. Rodriguez, M. E. Ramirez, and R. Paris, Nonequilibrium thermal entanglement, Phys. Rev. A **75**, 032308 (2007).

[17] I. Sinaysky, F. Petruccione, and D. Burgarth, Dynamics of nonequilibrium thermal entanglement, Phys. Rev. A **78**, 062301 (2008).

[18] M. Aspelmeyer, T. J. Kippenberg, and F. Marquardt, Cavity optomechanics, Rev. Mod. Phys. **86**, 1391 (2014).

[19] B. D. Hassard, B. D. Hassard, N. D. Kazarinoff, Y.-H. Wan, and Y. W. Wan, *Theory and Applications of Hopf Bifurcation* (CUP Archive, 1981).

[20] H. Grabert, Nonlinear relaxation and fluctuations of damped quantum systems, Z. Phys. B **49**, 161 (1982).

[21] H. C. Öttinger, Nonlinear thermodynamic quantum master equation: Properties and examples, Phys. Rev. A **82**, 052119 (2010).

[22] H. C. Öttinger, The geometry and thermodynamics of dissipative quantum systems, Europhys. Lett. **94**, 10006 (2011).

[23] V. I. Yukalov, Nonlinear spin dynamics in nuclear magnets, Phys. Rev. B **53**, 9232 (1996).

[24] G. A. Prataviera and S. S. Mizrahi, Many-particle Sudarshan-Lindblad equation: Mean-field approximation, nonlinearity and dissipation in a spin system, Rev. Bras. Ensino Física **36**, 01 (2014).

[25] T. Yu and J. H. Eberly, Quantum Open System Theory: Bipartite Aspects, Phys. Rev. Lett. **97**, 140403 (2006).

[26] N. Alfasi, S. Masis, O. Shtempluck, and E. Buks, Detection of paramagnetic defects in diamond using off-resonance excitation of NV centers, Phys. Rev. B **99**, 214111 (2019).

[27] M. W. Doherty, N. B. Manson, P. Delaney, F. Jelezko, J. Wrachtrup, and L. C. L. Hollenberg, The nitrogen-vacancy color center in diamond, Phys. Rep. **528**, 1 (2013).

[28] R. J. Cook and D. H. Whiffen, Electron nuclear double resonance study of a nitrogen center in diamond, Proc. R. Soc. London, Ser. A **295**, 99 (1966).

[29] L. Robledo, H. Bernien, T. van der Sar, and R. Hanson, Spin dynamics in the optical cycle of single nitrogen-vacancy centres in diamond, New J. Phys. **13**, 025013 (2011).

[30] D. A. Redman, S. Brown, R. H. Sands, and S. C. Rand, Spin Dynamics and Electronic States of N-*V* Centers in Diamond by EPR and Four-Wave-Mixing Spectroscopy, Phys. Rev. Lett. **67**, 3420 (1991).